

OUTFLOWS AT THE EDGES OF ACTIVE REGIONS: CONTRIBUTION TO SOLAR WIND FORMATION?

L. K. HARRA,¹ T. SAKAO,² C. H. MANDRINI,³ H. HARA,⁴ S. IMADA,⁴ P. R. YOUNG,⁵ L. VAN DRIEL–GESZTELYI,¹ AND D. BAKER¹

Received 2008 January 28; accepted 2008 February 13; published 2008 March 12

ABSTRACT

The formation of the slow solar wind has been debated for many years. In this Letter we show evidence of persistent outflow at the edges of an active region as measured by the EUV Imaging Spectrometer on board *Hinode*. The Doppler velocity ranged between 20 and 50 km s⁻¹ and was consistent with a steady flow seen in the X-Ray Telescope. The latter showed steady, pulsing outflowing material and some transverse motions of the loops. We analyze the magnetic field around the active region and produce a coronal magnetic field model. We determine from the latter that the outflow speeds adjusted for line-of-sight effects can reach over 100 km s⁻¹. We can interpret this outflow as expansion of loops that lie over the active region, which may either reconnect with neighboring large-scale loops or are likely to open to the interplanetary space. This material constitutes at least part of the slow solar wind.

Subject headings: solar wind

Online material: color figure

1. INTRODUCTION

The Sun produces persistent winds—both slow (≈ 300 km s⁻¹) and fast (≈ 800 km s⁻¹). Although it is now well established that the fast solar wind emanates from the coronal holes, it is not as clear from where the slow solar wind originates. Various sources have been suggested such as the boundary of coronal holes, helmet streamers (which are thought to delineate the closed and open corona), and the edges of active regions. Linking up with in situ measurements has also provided good insight. However, there is debate over whether active regions (outside of eruptions) contribute to the slow solar wind. Evidence for open field lines and expanding loops has been found by many authors, e.g., Švestka et al. (1977), Levine et al. (1977), Uchida et al. (1992), and Liewer et al. (2004). However there is some dispute over this by Švestka & Fárník (2005), whose study suggested that active regions could not be a permanent source of the slow solar wind.

The *Transition Region and Coronal Explorer (TRACE)* observed an active region in high cadence and measured persistent and intermittent outflows with projected velocities of between 5 and 20 km s⁻¹ (Winebarger et al. 2001). There is no obvious periodicity in this observation and hence they concluded that the flows are a class of reconnection events. Recent observations with the X-Ray Telescope (XRT) on board *Hinode* have demonstrated continuous outflow of soft X-ray plasma along extended large-scale loops (Sakao et al. 2007). They determine that this source could make up a good fraction of the slow solar wind. In this Letter we look in more detail at the same active region, using XRT and also the EUV Imaging Spectrometer to determine whether there are any spectroscopically measured outflows, and study the magnetic field configuration

to determine whether it is possible to produce such “open” magnetic field.

2. OBSERVATIONS

Hinode is a Japanese/US/UK mission (Kosugi et al. 2007), which was launched in 2007 September. It consists of a suite of three instruments that observe the Sun from the photosphere to the corona: the Solar Optical Telescope (SOT), the X-Ray Telescope (XRT), and the EUV Imaging Spectrometer (EIS).

The EIS instrument (Culhane et al. 2007) has two wave bands: 166–211 Å and 246–292 Å. It has four slit/slot positions: 1”, 2”, 40”, and 266”, allowing a wide choice of modes of operation. The EIS observations in this Letter were made with the 2” slit and carried out by “rastering” over 120 positions to build up an image. The observations started on 2007 February 20 at 23:45 UT lasting 13 minutes. We calibrated the data using the SolarSoft routine `eis_prep` and fitted a Gaussian profile to the spectral profiles in order to measure the Doppler velocity and line width. The slit tilt and the orbital variation effect were removed using the `eis_wave_corr` routine. The line profiles of the Fe XII 195 Å spectral line were fitted with simple Gaussian profiles.

XRT is a grazing incidence soft X-ray imager that achieves high angular resolution ($\approx 1''$) with a broad temperature coverage (Golub et al. 2007). XRT was observing mostly with the titanium-on-polyimide (Ti_poly) filter, with the readout size on the CCD being 512 × 512 pixels.

The Michelson Doppler Imager (MDI; Scherrer et al. 1995) on board *SOHO* images the Sun on a 1024 × 1024 CCD camera through a series of increasingly narrow filters. The final elements, a pair of tunable Michelson interferometers, enable MDI to record filtergrams with a FWHM bandwidth of 100 mÅ. In this Letter we analyze 5 minute averaged magnetograms of the full disk with a 96 minute cadence and a pixel size of 1.98”.

3. RESULTS

The active region seen in X-rays is shown in Figure 1. The region of interest is at the northeast edge of the active region where steady outflow is seen in XRT over a period of several days (as discussed in Sakao et al. 2007). Figure 1 also shows

¹ UCL–Mullard Space Science Laboratory, Holmbury St. Mary, Dorking, Surrey RH5 6NT, UK; lkh@mssl.ucl.ac.uk.

² Institute of Space and Astronautical Science, Japan Aerospace Exploration Agency, 3-1-1 Yoshinodai, Sagami-hara, Kanagawa 229-8510, Japan.

³ Instituto de Astronomía y Física del Espacio, CONICET-UBA, CC. 67, Suc. 28, 1428 Buenos Aires, Argentina.

⁴ National Astronomical Observatory of Japan, Mitaka, Tokyo 181-8588, Japan.

⁵ STFC Rutherford Appleton Laboratory, Chilton, Didcot, Oxfordshire OX11 0QX, UK.

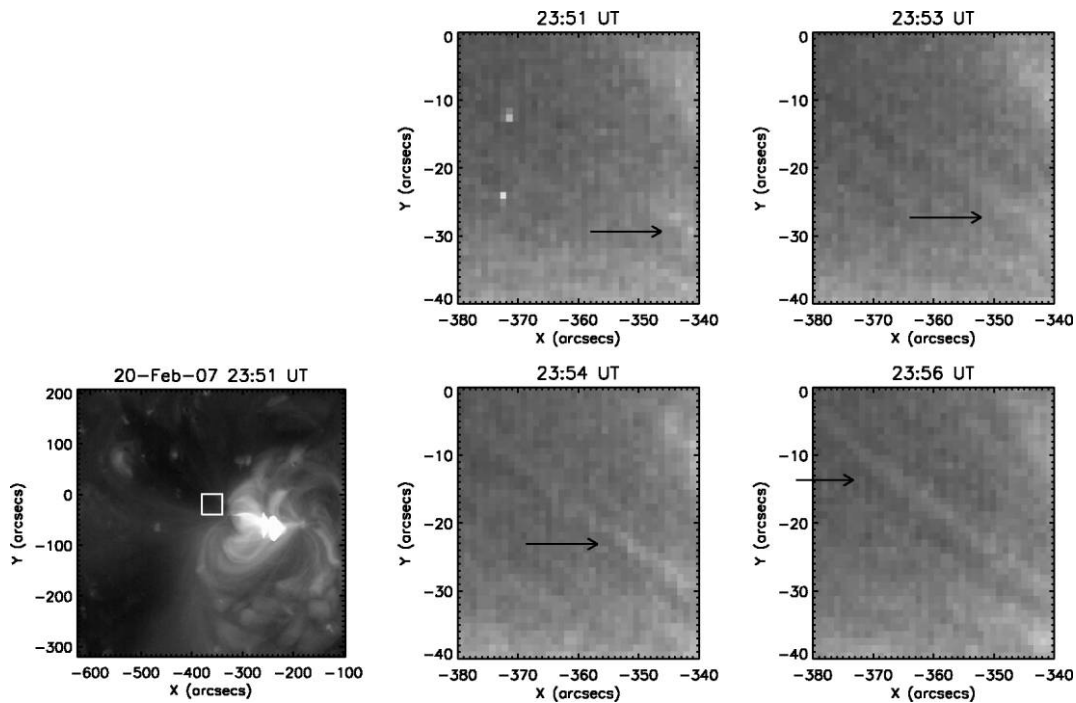


FIG. 1.—Left-hand panel shows a XRT (Ti_{poly}) image with a box highlighting the area to be enlarged. Right-hand panels show the progression of plasma along a loop with arrows highlighting the progress. The velocity of propagation is approximately 90 km s^{-1} .

a magnified portion of the region of interest over a period of 5 minutes. The arrows point to a loop that appears to be filled with hot plasma in the time period of minutes. The velocity of this “flow” of plasma is $\approx 90 \text{ km s}^{-1}$.

Figure 2 shows observations from EIS. The intensity map in the 195 \AA emission line is shown on the left (in a logarithmic scale) and the right shows the Doppler velocity map. The velocity map was obtained by single Gaussian fitting to the line profiles. The region of interest in the northeast of the active region shows weak emission that appears to be long loops. These loops show steady outflows of between 20 and 50 km s^{-1} with the strongest outflow toward the footpoints of the loops. As has been seen before, often with EIS, the weakest and potentially least interesting regions show the strongest flows and largest line widths (e.g., Doschek et al. 2007; Imada et al. 2007).

In order to determine what is the origin of the flows we

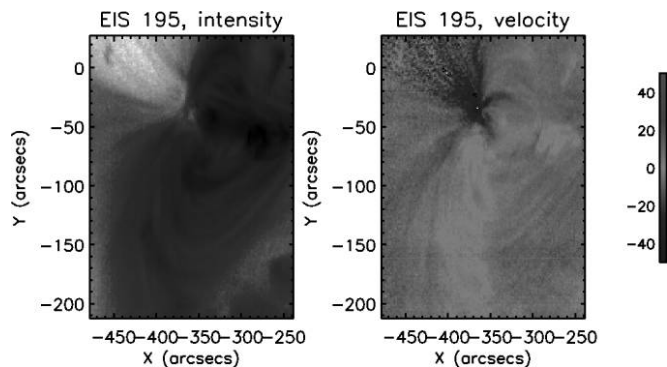


FIG. 2.—Left panel shows the intensity map in the 195 \AA line from EIS. Right panel shows the Doppler velocity measurements. The raster starts at 23:45 UT on 2007 February 20. [See the electronic edition of the Journal for a color version of this figure.]

analyze the magnetic field in the AR and its surroundings. Figure 3 shows the XRT image with MDI magnetic field contours, levels of ± 100 and 200 G . As can be seen to the east (*left-hand side*) of the AR there is an area of weak positive magnetic field, which appears to be a small coronal hole. The coronal hole has the same polarity as the eastern side of the AR and, hence, it is not likely that magnetic reconnection could occur between loops anchored at the AR edge and at the coronal hole.

On the western side of the AR there is a much smaller extended bipole. This has small loops which connect it to the AR (see Fig. 3). A large-scale potential magnetic field model (obtained as discussed in the next paragraph with $\alpha = 0$) shows that field lines at the eastern AR edge (see Fig. 5), that might correspond to the outer loops in Figure 2 and 3 are very extended. It is difficult to determine whether the loops with the outflow are “open” to the interplanetary medium or are large expanding loops; comparing them to the large-scale extrapo-

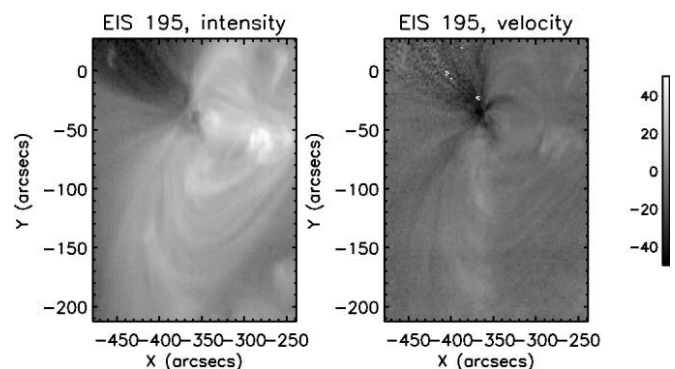


FIG. 3.—XRT image in the Ti_{poly} filter with the MDI magnetogram shown in contours. The contour levels are 100 and 200 with white showing the positive magnetic field. The white box shows the EIS field of view.

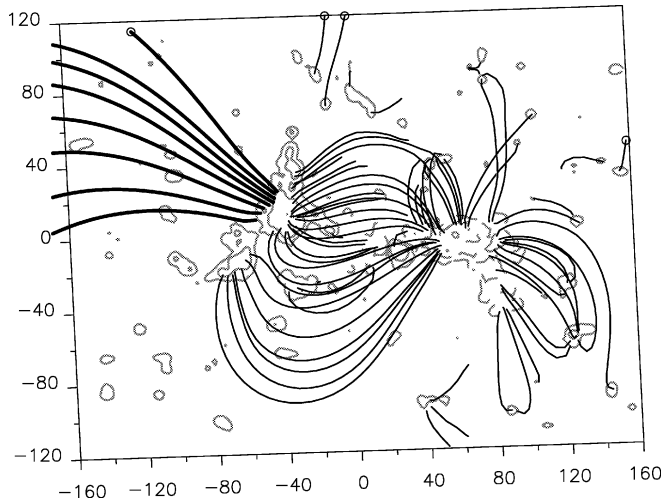


FIG. 4.—Magnetic field coronal model showing the active region and its surroundings. Contour levels are ± 50 , 100, and 500 G. The axes are in Mm. The thicker lines shown are calculated with $\alpha = 0$ and the other field lines have been fitted to have an $\alpha = 9.4 \times 10^{-3} \text{ Mm}^{-1}$. The (0, 0) point is at heliographic units S11°E15°. The x -direction is 444" and the y -direction has a distance of 333".

lated lines, both are possibilities. If they are large expanding loops, and our extrapolated lines represent these loops, their other ends are at the western edge of the smaller bipole (negative polarity). EIS did observe this small bipole on 2007 February 22 at 00:14 UT, and we searched for evidence of upflows. There are some upflows at the western edge of the bipole with velocities of less than 10 km s^{-1} , which are not unusual, so we cannot conclusively demonstrate that both flows are related.

A small-scale model of the coronal magnetic field, centered at the AR solar disk heliographic coordinates, was also calculated. Using the MDI magnetogram shown in Figure 3 as the boundary condition, the coronal magnetic field was computed assuming a linear force-free field (i.e., $\nabla \times B = \alpha B$) with the code described in Démoulin et al. (1997), which is based on the fast Fourier transform method developed by Alissandrakis (1981). The free parameter of our magnetic field model, α , was determined so that the computed field lines match the observed XRT loops within the AR; this value is $\alpha = 9.4 \times 10^{-3} \text{ Mm}^{-1}$ for all field lines in Figure 4, except those anchored on the AR eastern edge, for which we are using $\alpha = 0$ as in Figure 5. These models have been combined in Figure 4 for better visualization with the potential field lines being shown as thicker lines. The two models are used to represent the different length scales involved at the active region level and also connecting active regions. Our model assumes a planar geometry and hence does not take into consideration the effect of curvature—this is more important for the larger scale model. However it is consistent with the observations so we are happy to accept this in this paper. More detailed modeling would be useful in the longer term.

Using the coronal field model we can determine the actual flow velocities (v), following the method described in Harra et al. (2004). Our main assumption is that the flows observed by EIS correspond to plasma flowing along the magnetic field lines, hence $v = v_l/B_l B$, where B is the magnetic field intensity and v_l and B_l are the line of sight velocity and magnetic field, respectively. The values of B/B_l , ranging from 1.2 to 2.5, are determined for the region of "open" field lines to the east of the AR. These B/B_l values yield a maximum velocity range of

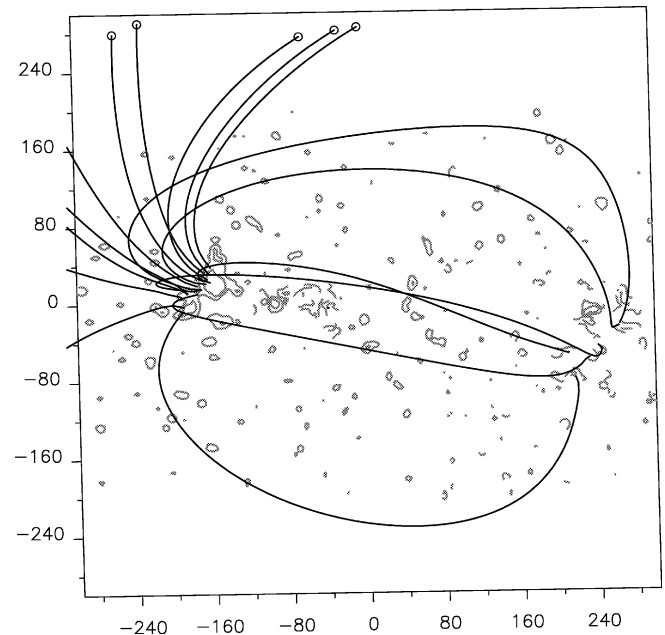


FIG. 5.—Large-scale coronal magnetic field model showing very extended field lines, some of them connecting the AR to the western bipole. Contour levels are ± 20 , 100, and 500 G. The axes are in Mm with (0, 0) being at heliographic position S11°E08°. The x -direction is 833" and the y -direction has a distance of 833".

60–125 km s^{-1} for the lower parts of the large-scale loops. This is consistent with the flow determined from the XRT images (90 km s^{-1}).

4. DISCUSSION

The source of the slow solar wind has been debated for many years with solutions such as helmet streamers, expanding active region loops, and the boundaries of coronal holes being options. In this Letter we are able to study a probable source region spectroscopically in order to see where the outflowing regions are. In this example we have an active region located between a positive polarity coronal hole and a weak extended bipole. Outflowing plasma is seen with both the XRT and EIS with the fastest speeds being close to the footpoints. The outflow is seen dominantly to the east side of the active region where the emission is weak. Weak emission is to be expected as the plasma is actually leaving the Sun. Indeed the propagation is also seen in the XRT data. The large-scale magnetic field model in Figure 5 shows that all the large loops at the eastern side of the AR are highly extended, reaching heights of 400–600 Mm for the closed loops connecting to the negative polarity of the smaller western bipole, while others are likely open to the interplanetary space.

The cause of the opening of the field lines is unclear. There is a small coronal hole on one side of the active region and an extended bipole on the other. Although evidence of active region interaction with coronal holes has been observed before (e.g., Baker et al. 2007), the magnetic configuration in this case does not seem favorable and there are no obvious signs of coronal hole interaction (such as a change in the coronal hole boundary). Another possibility is that we are observing loop expansion. Uchida et al. (1992) found observational evidence of this in *Yohkoh* data where the corona above active regions was found to expand continuously. Our observations show per-

sistent flows over the time period of days. We also observe many small-scale brightenings to the western edge (*right-hand side*) of the AR. These brightenings or short loops, modeled in Figure 4, are suggestive of being signatures of reconnection with the neighboring extended bipole. This magnetic reconnection process also creates a set of long external loops that would correspond to the large-scale lines anchored at the eastern edge of the AR and the negative polarity of the extended bipole in Figure 5. These set of reconnected loops is expected to expand in order to reach equilibrium (Priest & Forbes 2000). The strong outflow on the east side of the AR is plausibly an outflow in such long reconnected and expanding loops.

The outflow we observe most likely forms part of the slow solar wind. Solar wind outflow has been observed through spectroscopic observations of the inner corona (*SOHO* UVCS) and in situ measurements such as those on the *ACE* spacecraft. Ko et al. (2006) used such data sets to study the abundance variation at the vicinity of an active region that was close to a coronal hole. Their analysis supports the idea that one source of the slow solar wind is the boundary region between the coronal hole and active region. This is also consistent with the work carried out by Kojima et al. (2000) who used interplanetary scintillation (IPS) data and found that the slow solar wind does not arise from the expanding closed active region loops, but from the vicinity of one polarity to the side of the active region. However, other work suggests that the source is the active region. This is also consistent with work by Kojima et al. (2000) who compared IPS data with Fe XIV data from ground-based observatories. Hick et al. (1995) found by linking interplanetary scintillation measurement for a period of a year that these match active regions significantly closer than the heliospheric current sheet which suggests that active regions

are not closed structures but provide input to the slow solar wind.

The large flows observed in this Letter could also have implications for the general structure of the plasma and coronal heating models. Aschwanden (2001) carries out an excellent review of current models and how they relate to observations. He concludes that plasma is continuously filling the corona from the chromosphere. He also points out that loops often look brighter than expected. Petrie (2006) looked at the impact of steady flows in loops and predicts that a flow of 100 km s⁻¹ can make loops look much brighter than expected. In addition, the work by Imada et al. (2007) shows a clear relationship between the outflow velocity and temperature above 1 MK, which again leans toward a broader linkage to the coronal heating mechanism.

In this example we show spectroscopic evidence for outflow from the edge of the active region which seems to be consistent with the expanding active region loops described by Uchida et al. (1992). Long-term studies are required linking up with interplanetary data sets to understand this further.

Hinode is a Japanese mission developed and launched by ISAS/JAXA, collaborating with NAOJ as a domestic partner, NASA and STFC (UK) as international partners. Scientific operation of the *Hinode* mission is conducted by the *Hinode* science team organized at ISAS/JAXA. This team mainly consists of scientists from institutes in the partner countries. Support for the postlaunch operation is provided by JAXA and NAOJ (Japan), STFC (UK), NASA, ESA, and NSC (Norway). We are grateful to the anonymous referee for improving the clarity of the Letter.

REFERENCES

- Alissandrakis, C. E. 1981, *A&A*, 100, 197
 Aschwanden, M. J. 2001, *ApJ*, 560, 1035
 Baker, D., van Driel-Gesztelyi, L., & Attrill, G. D. R. 2007, *Astron. Nachr.*, 328, 773
 Culhane, J. L., et al. 2007, *Sol. Phys.*, 243, 19
 Démoulin, P., Henoux, J. C., Mandrini, C. H., & Priest, E. R. 1997, *Sol. Phys.*, 174, 73
 Doschek, G. A., et al. 2007, *ApJ*, 667, L109
 Golub, L., et al. 2007, *Sol. Phys.*, 243, 63
 Harra, L. K., Mandrini, C. H., & Matthews, S. A. 2004, *Sol. Phys.*, 223, 57
 Hick, P. L., Jackson, B. V., Rappaport, S., Woan, G., Slater, G., Strong, K., & Uchida, Y. 1995, *Geophys. Res. Lett.*, 22, 643
 Imada, S., Hara, H., Watanabe, T., Kamio, S., Asai, A., Matsuzai, K., Harra, L. K., & Mariska, J. T. 2007, *PASJ*, 59, S793
 Ko, Y.-K., Raymond, J. C., Zurbuchen, T. H., Riley, P., Raines, J. M., & Strachan, L. 2006, *ApJ*, 646, 1275
 Kojima, M., Fujiki, K., Hakamada, K., Ohmi, T., Tokumaru, M., & Yokobe, A. 2000, *Adv. Space Res.*, 25, 1893
 Kosugi, T., et al. 2007, *Sol. Phys.*, 243, 3
 Levine, R. H. 1977, *ApJ*, 218, 291
 Liewer, P. C., Neugebauer, M., & Zurbuchen, T. 2004, *Sol. Phys.*, 223, 209
 Petrie, G. J. D. 2006, *ApJ*, 649, 1078
 Priest, E., & Forbes, T. 2000, *Magnetic Reconnection* (Cambridge: Cambridge Univ. Press)
 Sakao, T., et al. 2007, *Science*, 318, 1585
 Scherrer, P. H., et al. 1995, *Sol. Phys.*, 162, 129
 Švestka, Z., & Fárnik, F. 2005, *Sol. Phys.*, 229, 305
 Švestka, Z., Solodyna, C. V., Howard, R., & Levine, R. H. 1977, *Sol. Phys.*, 55, 359
 Uchida, Y., McAllister, A., Strong, K. T., Ogawara, T., Shimizu, T., Matsumoto, R., & Hudson, H. S. 1992, *PASJ*, 44, L155
 Winebarger, A. R., DeLuca, E. E., & Golub, L. 2001, *ApJ*, 553, L81